Proceedings of the
Annual Stability Conference
Structural Stability Research Council
Atlanta, Georgia, April 21-24, 2026

Damage detection and sensor optimization for stability characterization of a meter-scale origami pill-bug structure

Ann C. Sychterz[1]

Abstract

Deployable structures have gained significant attention in engineering due to their adaptive capabilities and potential applications in various fields. This work focuses on the Origami Pill Bug, a novel deployable origami structure, for investigating the behavior of origami-inspired deployable systems under damage scenarios. Using an optimized sensor array, strain data is collected during deployment of the structure in both damaged and undamaged states. Damage classification is achieved through supervised machine learning techniques - Support Vector Machines, Random Forest, and K-Nearest Neighbors - with effect size features derived from strain variation serving as inputs. A comparative evaluation of these models is conducted using classification accuracy to determine the most suitable algorithm for damage classification. The study provides a framework for enhancing structural health monitoring in deployable origami structures, paving the way for improved safety and maintenance protocols.

Keywords: Origami, damage detection, life cycle assessment, machine learning

1. Introduction

Deployable structures, with their ability to undergo large scale reconfiguration, offer a promising avenue for sustainable infrastructure development. Their versatility extends beyond aerospace applications (Pellegrino, 1995), holding promise for the civil engineering sector as well. However, their deployable nature introduces geometrically non-linear behavior and large displacements, posing challenges for conventional design tools (Gantes et al., 1989). Due to the application-specific nature of these adaptive structures, there is a pressing need to investigate structural health monitoring methods that can effectively assess their condition and facilitate broader implementation in civil engineering applications.

Origami's influence on engineering design has gained significant traction, inspiring diverse structures from deployable solar panels (Miura et al., 1985) to self-assembling stents and configurable materials. This influence extends beyond simple foldability, as the understanding of origami geometry has been leveraged to design rigid-foldable structures and even provide insight into the kinematics of folded metamaterials (Schenk & Guest, 2013). However, while modeling

[1] Assistant Professor, University of Illinois Urbana-Champaign, <asychter@illinois.edu>

approaches using pin-jointed bars offer valuable insights, bridging the gap between theoretical models and real-world applications remains a challenge.

Machine learning has emerged as a powerful tool for damage classification in deployable structures, addressing the challenges posed by their unique folding, unfolding, and reconfigurable nature. Supervised learning techniques, such as Support Vector Machines (SVM), Random Forests (RF), and k-Nearest Neighbors (KNN), have been widely applied to classify structural damage based on features extracted from strain or vibration responses. Although deep learning methods like Convolutional Neural Networks (CNNs) demonstrate high accuracy in damage classification tasks, their demand for large datasets and computational resources limits their applicability in deployable systems. The choice of algorithm depends on factors such as dataset size, complexity of damage patterns, and computational constraints (An et al., 2015), highlighting the need for tailored approaches that account for the dynamic characteristics of deployable structures.

The goal of this study is to develop and evaluate a robust framework for damage detection and classification in deployable structures, using the Origami Pill Bug (OPB) as a case study. By combining statistical strain analysis and advanced supervised machine learning techniques, this research aims to accurately identify and classify structural damage scenarios using a fixed sensor array. The study addresses key challenges unique to deployable structures, such as limited sensor placement options and dynamic boundary conditions, while leveraging machine learning algorithms like Support Vector Machines (SVM), Random Forest (RF), and k-Nearest Neighbors (KNN) to analyze strain profile variations. Ultimately, this work seeks to enhance the reliability and resilience of deployable systems, contributing to the broader field of structural health monitoring and paving the way for intelligent infrastructure solutions in adaptive engineering applications.

2. Methodology

The following sections present the design and construction of a meter-scale Origami Pill Bug prototype (Figure 1), along with the actuation mechanism. It details the fabrication process using precision laser cutting and the incorporation of lockable brackets and hinges for folding. Measurement metrics like planar length and percentage rolling are defined, which are used to quantify the prototype's deployment.

The development of the final meter-scale prototype was preceded by an iterative process of design refinement and testing. Multiple prototypes were developed and evaluated, each iteration providing valuable insights and improvements. These preliminary versions allowed for the identification and resolution of design challenges, optimization of folding mechanisms, and refinement of actuation systems.

The final meter-scale prototype is fabricated from 0.635 cm thick hardwood panels, with an elastic modulus of 16,428 MPa and a yield strength of 80.65 MPa. The flat-folded prototype measures 100 cm in length and 40 cm in width, with a net mass of 6.4 kg. Leveraging a 60-Watt laser cutter (Universal Laser VLS4.60) ensures dimensional accuracy and minimizes manufacturing errors through precise panel cutting and screw hole placement. The material properties of the prototype are listed in Table 1.

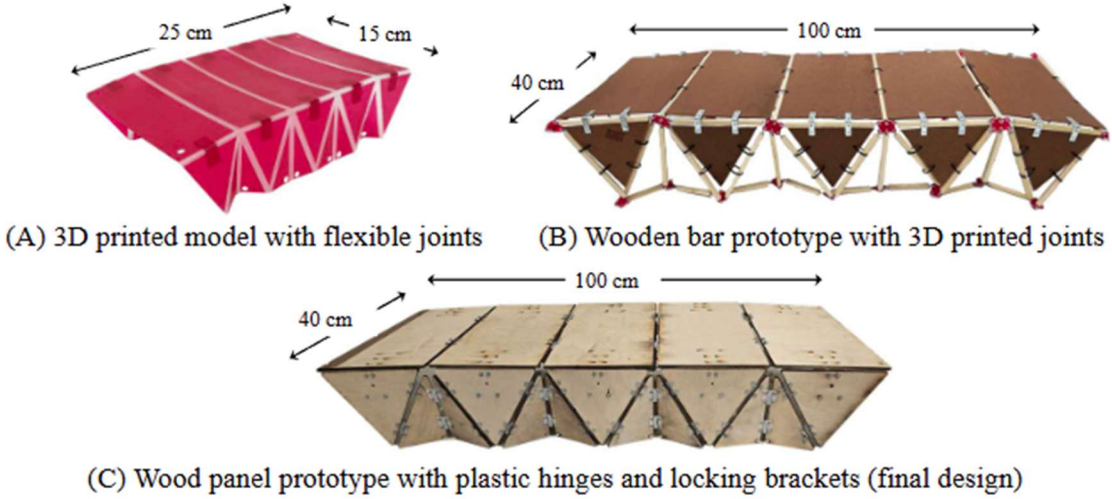

Figure 1: Prototype iterations: (A) 3D printed model with flexible joints, (B) Wooden bar prototype with 3D printed joints, and (C) Wood panel prototype with plastic hinges and locking brackets (final design)

Table 1: Origami Pill Bug Meter-Scale Model Properties

Property	Values	
Young's Modulus, $\boldsymbol{E}$	16,428	MPa
Yield Strength, $\boldsymbol{\sigma_y}$	80.65	MPa
Density, $\boldsymbol{\gamma}$	306	kg/m^3
Poisson's Ratio, $\boldsymbol{\nu}$	0.3	
Plate Thickness, $\boldsymbol{T_p}$	0.635	cm

The investigation utilized the meter-scale prototype of the OPB equipped with an optimized fixed sensor array of seven strain sensors (Figure 2). A National Instruments compact data acquisition system recorded strain data during deployment at 200 Hz sampling rate. Five distinct cases are examined: a healthy (H) case and four damage cases (DC1-DC4), each corresponding to damage of one Type-C panel in the OPB as shown in Figure 3 (A). To replicate the damage event in the OPB prototype, a damaged panel of Type-C is specifically designed (Figure 3 (B)). For each damage case, the corresponding intact panel is replaced with this damaged panel. Strain development is then recorded throughout deployment of the OPB prototype. To ensure statistical robustness, 20 iterations of readings are conducted for each case, resulting in a dataset of 100 total readings.

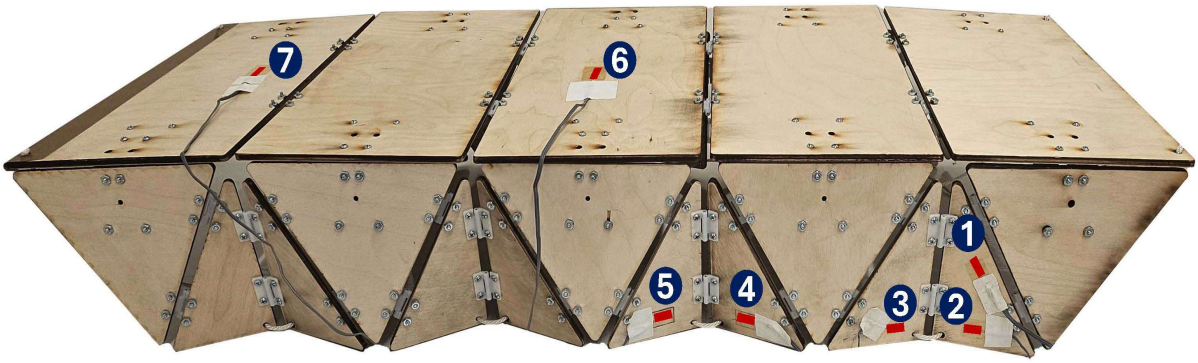

Figure 2: Placement of seven strain sensors (1-7) on meter-scale OPB prototype.

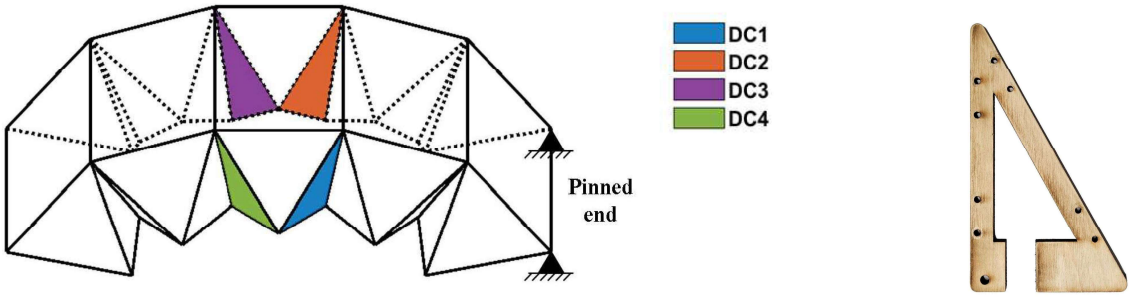

(A) Damage Cases (B) Damaged Panel Type-C

Figure 3: (A)Visualization of the OPB structure highlighting the damaged panels for damage case: DC1 (blue), DC2 (orange), DC3 (purple), and DC4 (green).(B) Design of the damaged panel of Type-C used to replicate damage events in the OPB prototype.

2.1 Statistical analysis and machine learning approach

The Mann-Whitney U test is employed to determine statistical significance of differences between the strain readings of the healthy and damage cases. Effect sizes are calculated using Rosenthal's r correlation coefficient to quantify the magnitude of observed differences according to the formula:

$$\boldsymbol{r} = \frac{\boldsymbol{Z}}{\sqrt{\boldsymbol{Ns}}} \tag{1}$$

where $\boldsymbol{Z}$ is the z-statistic from the Mann-Whitney U test and $\boldsymbol{Ns}$ is the total sample size. For damage classification, three supervised machine learning algorithms were implemented: Support Vector Machines (SVM) with Radial Basis Function kernel, Random Forest (RF), and K-Nearest Neighbors (KNN) with cosine distance metric. The models are trained on a dataset consisting of input features (effect sizes) and corresponding output labels (damage case labels). The goal is for the models to learn the mapping between the input space of effect sizes and the output space of case labels. Data augmentation techniques, such as Gaussian noise addition and feature scaling, enhanced model robustness and increased dataset size. A 5-fold cross-validation strategy assessed model performance, with iterative hyperparameter tuning over 50 iterations to optimize accuracy.

2.2 Life cycle assessment

In the context of emergency shelters, the deployable Origami Pill Bug (OPB) is proposed as a sustainable alternative to typical wood structures. Focusing on emergency shelters highlights an area where environmental impact and resource efficiency can yield particularly meaningful benefits. Emergencies often call for immediate, large-scale deployments, which magnify the overall carbon footprint. Improvements achieved through design optimization, resource conservation, or reusability thus translate to significant reductions in greenhouse gas emissions at scale. Additionally, these structures are typically prefabricated in controlled plant environments to ensure consistency in quality. Therefore, the logistical and infrastructural constraints of emergency contexts make transportation efficiency crucial, as it can significantly impact both cost and emissions. By contrasting the deployable OPB concept with the typical shelter, the analysis underlines how structural innovation can transform the typical resource-intensive approach to emergency shelter deployment.

This study presents a comparative life cycle analysis (LCA) of two emergency shelter designs: a typical single-use structure (Figure 4(A)) and a deployable Origami Pill Bug (OPB) structure (Figure 4 (B)). This comparison leads to an assessment of whether performance improvements of the deployable shelter design in terms of environmental impact can offset increased energy costs from its actuation. This also aligns with efforts by international humanitarian coordination mechanisms to advance and support partners in reducing the environmental impact of shelter responses.

The functional unit for this study is defined as a temporary shelter designed for a maximum of 4 occupants, with a floor area of 14 m^2, intended for emergency use over a six-month period. The occupiable interior volume for both shelters is 37 m^3, ensuring sufficient spatial capacity to meet basic living requirements in emergency scenarios. This ensures a fair comparison between the typical wood shelter and the deployable shelter, focusing on their primary function of providing adequate living space for displaced individuals in crisis situations. This study employs a cradle-to-grave approach for LCA. The system boundary is illustrated in Figure 5, which shows the stages and processes included in the life cycle analysis of the typical OPB shelters.

(A) Typical wood structure. (B) Deployable OPB structure.

Figure 4: (A) Typical wood structure, and (B) Deployable OPB structure for emergency shelters.

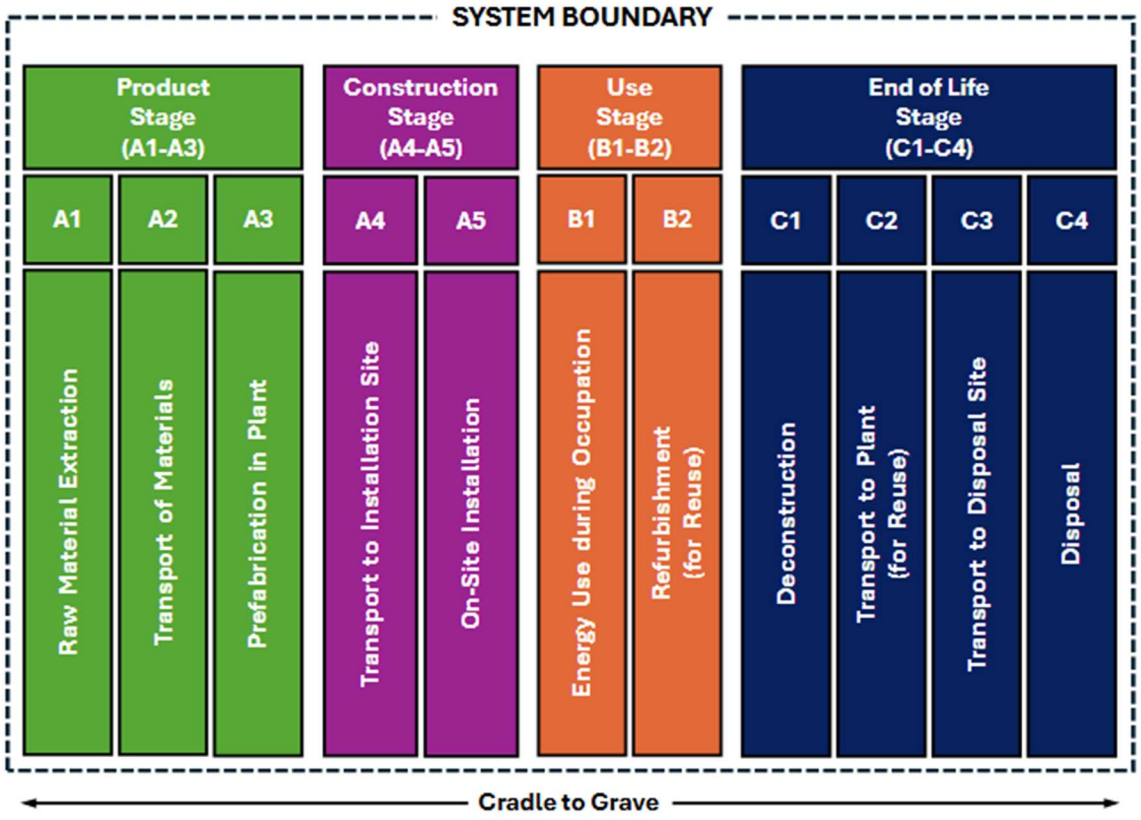

Figure 5: Stages and processes for LCA.

The following foundational assumptions underpin this study:

- Although the OPB structure is not completely enclosed, both designs meet minimum humanitarian standards for emergency shelter, including structural integrity and basic habitability, with a designed usable life of six months for a single use cycle.
- Energy use in the six-month operational period is assumed to be the same for both structures due to limited variability in operational factors within emergency settings.
- Both structures are prefabricated, acknowledging the benefits of consistent manufacturing conditions at the plant, while also accounting for the potential logistical and infrastructural limitations typically associated with installation site.
- Packing efficiency is accounted for by calculating the volume each structure occupies in a standard 50m^3 truck after prefabrication. The typical structure occupies 78\% and the OPB structure occupies 25.6\% of the truck volume.
- Transportation distances are assumed to be equal for both shelter types, focusing on inherent material and design differences.
- The typical structure is assumed to be disposed of entirely after a single use, with no potential for recycling or reuse.
- The maintenance requirement between each consecutive deployment is assumed to be consistent for the deployable OPB structure, with each refurbishment cycle involving a standardized 20\% material replacement to restore operational integrity.

The OPB structure is considered for five use cycles, as the 20\% material replacement per refurbishment cycle effectively results in a complete material replacement over the course of these cycles.

3. Results

3.1 Statistical analysis and machine learning approach

The SVM classifier consistently outperformed both RF and KNN, with its accuracy reaching nearly 100% by the 43rd iteration of parameter tuning. The Random Forest classifier stabilized around 98% accuracy, while KNN showed limited improvement, reaching approximately 83% maximum accuracy as shown in Figure 6. The final SVM model demonstrated 100% accuracy across all five when tested on 50 new samples.

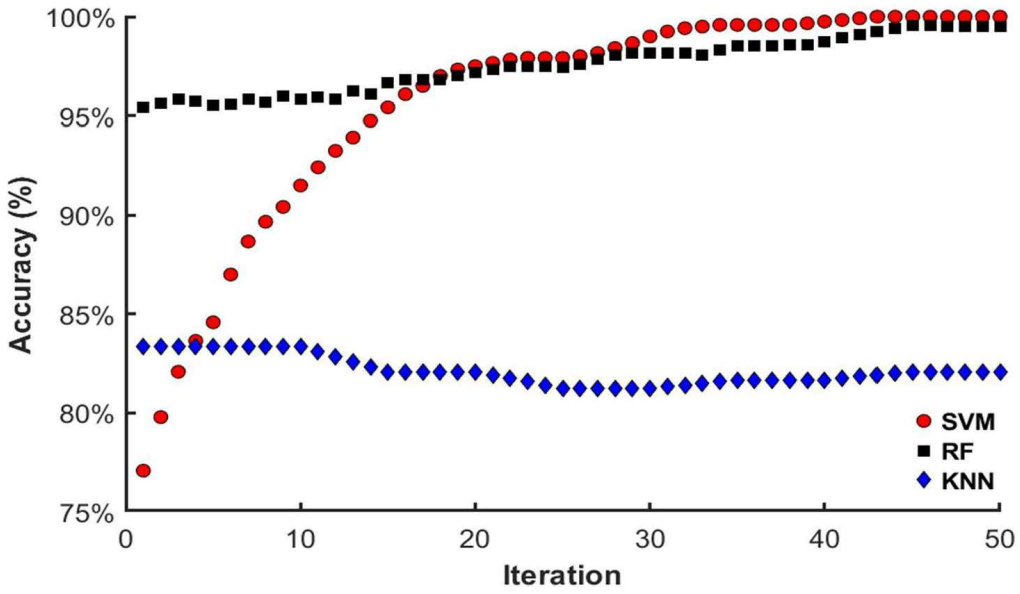

Figure 6: Classification accuracy over iterations for three classification models: SVM, RF, and KNN.

3.2 Life cycle assessment

The life cycle inventory data was calculated for each shelter type and scenario and summarized in Table 2. Embodied energy, which includes the total energy consumed in material extraction, production, transport, maintenance, and end-of-life processes makes up the majority of the environmental impact for both shelter types across all three scenarios. Operational energy, which represents energy use during the six-month occupancy phase, remains the same across all three scenarios at 651.87 kg CO2 eq. However, its contribution to the total GWP varies depending on the shelter type and use cycle. For the typical shelter, embodied energy accounts for 86% of the total GWP, with operational energy contributing 14%. In the single-use OPB shelter, embodied energy makes up 78% of the GWP, while operational energy represents 22%. In the multi-cycle scenario for the OPB shelter, embodied energy decreases further to 57% of the total GWP, while operational energy increases to 43%, resulting in the lowest overall GWP among the scenarios. This analysis shows that the primary reduction in GWP across the scenarios is due to decreases in embodied energy, emphasizing the impact of material efficiency, transportability and reusability.

These findings emphasize the potential of innovative design strategies, such as the OPB shelter, to significantly reduce the environmental impact of buildings. This analysis serves as a foundation for future developments in deployable origami-inspired structures, advocating for designs that minimize both initial footprints and lifecycle emissions.

Table 2: Life Cycle Inventory for Typical and OPB Structures

Process	Unit	Typical	OPB
A1 Raw Material Extraction			
Wood (Pine)	m^3	1.8	0.6
Steel	kg	0.8	76.7
Polyethylene (High Modulus Polyethylene)	kg	-	4.6
Plastic (High-Impact Acrylic with Urethane Elastomer)	kg	-	42.0
Paint (solvent based)	kg	32.6	11.7
A2 Transport of Materials			
Wood (Pine)	km	200.0	200.0
Steel	km	150.0	150.0
Polyethylene (High Modulus Polyethylene)	km	-	100.0
Plastic (High-Impact Acrylic with Urethane Elastomer)	km	-	100.0
Paint (solvent based)	km	50.0	50.0
A3 Prefabrication in Plant	kWh	31.5	57.5
A4 Transport to Installation Site	km	150.0	150.0
A5 On-site Installation	kWh	5.8	6.3
B1 Energy Use during Occupation	kWh	360.0	360.0
B2 Refurbishment (for Reuse) - 20% Replacement			
Wood (Pine)	m^3	-	0.1
Steel	kg	-	15.3
Polyethylene (High Modulus Polyethylene)	kg	-	0.9
Plastic (High-Impact Acrylic with Urethane Elastomer)	kg	-	8.4
Paint (solvent based)	kg	-	2.3
Energy Use	kWh	-	11.5
C1 Deconstruction	kWh	7.8	8.3
C2 Transport to Plant (for Reuse)	km	-	150.0
C3 Transport to Disposal Site			
Wood (Pine)	km	75.0	75.0
Steel	km	100.0	100.0
Polyethylene (High Modulus Polyethylene)	km	-	150.0
Plastic (High-Impact Acrylic with Urethane Elastomer)	km	-	150.0
Paint (solvent based)	km	75.0	75.0
C4 Disposal			
Wood (Pine)	kg	897.8	308.9
Steel	kg	0.8	76.7
Polyethylene (High Modulus Polyethylene)	kg	-	4.6
Plastic (High-Impact Acrylic with Urethane Elastomer)	kg	-	42.0
Paint (solvent based)	kg	32.6	11.7

4. Discussion

Among the machine learning models, SVM demonstrated superior performance due to its ability to handle non-linear boundaries between classes. The iterative refinement of the regularization parameter contributed to improving the decision boundaries, leading to better generalization. The Random Forest model also performed well but was likely limited by its reliance on decision trees. KNN struggled due to the high dimensionality of the dataset, which increased the complexity of nearest-neighbor searches. The data augmentation and feature scaling techniques proved highly effective in improving model performance. By introducing noise and scaling, the models were able to generalize better to unseen data, with cross-validation ensuring robustness across different subsets of the data.

5. Conclusions

This study demonstrates the effectiveness of combining optimized sensor placement, statistical strain analysis, and machine learning techniques for damage detection and classification in deployable structures, using the Origami Pill Bug as a case study. Among the three supervised machine learning algorithms investigated, Support Vector Machines (SVM) achieved near-perfect accuracy, highlighting its suitability for handling non-linear class boundaries in limited datasets. The findings underscore the potential of this framework to enhance structural health monitoring by providing accurate damage detection capabilities using a fixed sensor array. This work not only advances the reliability and resilience of deployable systems but also lays a foundation for future research into adaptive engineering solutions and intelligent infrastructure systems. The deployable OPB design may involve assembly procedures that necessitate specialized training or tools, highlighting the importance of simplifying assembly processes or providing clear instructional support. The current deployable solution might face challenges in effectively integrating locally available materials and labor, suggesting a need to explore opportunities for local resource utilization and community involvement

Acknowledgements

This research was supported by funding provided by the Grainger College of Engineering at the University of Illinois Urbana-Champaign.

References

An, D., Kim, N. H., & Choi, J. H. (2015). Practical options for selecting data-driven or physics-based prognostics algorithms with reviews. *Reliability Engineering & System Safety*, *133*, 223–236. https://doi.org/10.1016/J.RESS.2014.09.014

Baruah, A. C., & Sychterz, A. C. (2025). Comparison of computational and experimental dynamic behavior of a meter-scale deployable origami pill bug structure. *Structures*, *71*, 108033. https://doi.org/10.1016/J.ISTRUC.2024.108033

Gantes, C. J., Connor, J. J., Logcher, R. D., & Rosenfeld, Y. (1989). Structural analysis and design of deployable structures. *Computers and Structures*, *32*(3–4), 661–669. https://doi.org/10.1016/0045-7949(89)90354-4

Miura, K., Furuya, H., & Suzuki, K. (1985). Variable geometry truss and its application to deployable truss and space crane arm. *Acta Astronautica*, *12*(7–8), 599–607. https://doi.org/10.1016/0094-5765(85)90131-6

Pellegrino, S. (1995). Large retractable appendages in spacecraft. *Journal of Spacecraft and Rockets*, *32*(6), 1006–1014. https://doi.org/10.2514/3.26722

Schenk, M., & Guest, S. D. (2013). Geometry of Miura-folded metamaterials. *Proceedings of the National Academy of Sciences of the United States of America*, *110*(9), 3276–3281. https://doi.org/10.1073/pnas.1217998110